Journal of Sound and Vibration 329 (2010) 961–972

Contents lists available at ScienceDirect

Journal of Sound and Vibration

journal homepage: www.elsevier.com/locate/jsvi

Independent modal control for nonlinear flexible structures: An experimental test rig

F. Resta, F. Ripamonti *, G. Cazzulani, M. Ferrari

Mechanical Engineering Department, Politecnico di Milano, Via La Masa, 1, 20186 Milano, Italy

ARTICLE INFO

Article history:
Received 21 July 2009
Received in revised form
11 September 2009
Accepted 15 October 2009
Handling Editor: A.V. Metrikine
Available online 17 November 2009

ABSTRACT

This paper investigates the use of independent modal control to suppress the vibration of nonlinear flexible structures. In recent years technological improvements in the mechanical field have led to high-performance systems with low weight and, as a consequence, high flexibility and low damping. Here active control quickly bettered the traditional passive damping systems. The structure investigated in this paper is a multi-body flexible boom moved by hydraulic actuators. The nonlinear system dynamic was numerically reproduced and a control strategy, based on the use of the same actuators, was developed. Finally a test rig was created to validate the proposed approach experimentally.

1. Introduction

In recent years vibration control has been increasingly used not only in aerospace research but also in many mechanical application fields. The need for weight reduction to improve system performance led to structures with high flexibility and low damping. These structures suffer fatigue and instability issues raising, as a consequence, a number of safety questions. Traditional external passive control methods are generally more invasive, introducing mass into the structure, and less effective in a large range of frequencies. On the other hand, active control is an attractive solution, especially considering the extensive development of calculator hardware and the consequent cost reduction. Among the different control techniques proposed in recent decades, modal control offers many advantages; thanks to its immediacy and connection to the dynamic design of the system. Moreover the improvement of sensor and actuator technology and innovative algorithms allows the spillover limits due to the truncated modes and unmodelled dynamic to be partly overcome.

In literature modal control was introduced by Balas [1] and Meirovitch [2] between the 1970s and 1980s. Balas' studies deal with vibration suppression in large spacecraft structures, applying the modal expansion theorem and modal control. Some years later Meirovitch proposed an independent modal space control (IMSC) using the modal filter technique for estimating the modal coordinates [3]. The method was further improved by Baz and Poh [4], who suggested a modified independent modal space control (MIMSC) for optimal gain calculation adopting piezoelectric actuators.

Anyway Lin and Chu [5] demonstrated that modal control, for a general dynamic system with complex mode shapes, does not assure stability even for the controlled modes. The spillover problems were partially cushioned by the use of distributed sensor and actuators [6] and some applications of IMSC for the control of flexible linkage mechanism [7,8] can be found. In 2001, Inman too [9] discussed the spillover issue associated with modal control, concluding that modern technology makes the problem manageable.

* Corresponding author. Tel.: +39 0223998480; fax: +39 0223998492.
E-mail address: francesco.ripamonti@polimi.it (F. Ripamonti).

0022-460X/$ - see front matter © 2009 Elsevier Ltd. All rights reserved.
doi:10.1016/j.jsv.2009.10.021

Moreover, modal control can be employed in conjunction with FEM for model definition, as shown by Skidmore [10] and Khulief [11]. They studied an active control scheme for vibration suppression in a single beam/cable structure, considering also its large motion. About this topic, to consider the deformability together with the system large motion, an interesting approach based on the fictitious loads was proposed by Lin [12].

This paper deals with independent modal control on a multi-body (MB) nonlinear flexible boom. In particular suppression of the vibration caused by the large motion of the structure was investigated. Because only a few modes actively participate in describing the system's dynamic behaviour, modal control is particularly useful.

The modal model required for the control law synthesis can be defined both experimentally, through a modal parameter identification campaign, or numerically, by means of FEM. In the proposed work the boom's FEM model is described. The model not only allowed control/observer gain to be defined through pole placement techniques, but also permitted numerical simulation. At the same time a test rig was created to validate the defined control law. A comparison between the behaviour with and without control is proposed, highlighting some considerations on spillover problems.

2. The system

The boom is composed of a number of segments, connected to each other with revolving joints (Fig. 1). Each segment's movement is generated by an hydraulic actuator through a kinematic chain assumed to be rigid.

Owing to the length and the low flexional stiffness of the section, the structure presents high flexibility producing, in normal operating conditions, low frequency vibrations, generally associated with a low damping ratio.

As previously mentioned, a numerical model was developed as a tool both for defining the control logic and for simulating boom behaviour. Initially a number of hypotheses were introduced:

- planar motion: the boom can be moved along two dimensions referred to as (x,y) below;
- small deformations: as a consequence a linear relationship between strains and deformations was considered. In addition, axial and bending deformations can be assumed to be decoupled; and
- small segment rotation speed: all centrifugal and Coriolis contributions can be neglected.

Thus this model has to be able to describe the large motion of the segments and their deformation due to flexibility. To write the motion equations, the following reference systems (Fig. 2) were defined:

- $(O-x,y)$ is the global boom reference system, sited on the boom base;
- (O^j-x^j,y^j) is the j-th segment's reference system; and
- $(O^{jk}-x^{jk},y^{jk})$ is the reference system of the k-th finite element of the j-th segment.

The boom kinematics were solved using the "floating frame of reference" formulation [13]. This formulation describes the motion as a sum of two contributions:

- the absolute displacement and rotation of the j-segment reference system (O^j-x^j,y^j) with respect to the absolute reference system $(O-x,y)$. The translation contribution can be written as a function of the degrees of freedom of the previous segments, while the rotation contribution is described by the independent variable θ^j; and

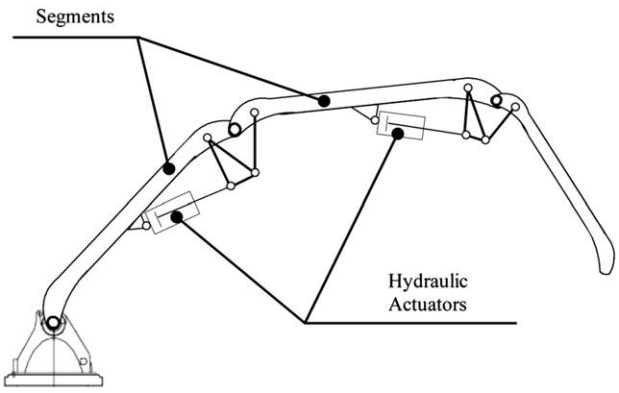

Fig. 1. Layout of the flexible boom.

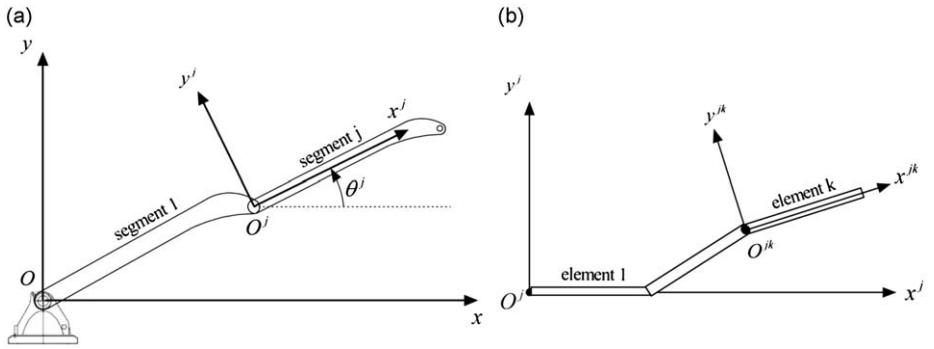

Fig. 2. Link reference systems (a) and finite element reference systems (b).

- the deformations of each segment with respect to its non-deformed configuration. This contribution is described, with the finite element method (FEM), using the vector $\underline{\mathbf{d}}$, that contains the three independent coordinates of each node.

As a consequence, the total independent variable vector can be defined as

$$\underline{\mathbf{z}} = \begin{Bmatrix} \underline{\boldsymbol{\theta}} \\ \underline{\mathbf{d}} \end{Bmatrix} \tag{1}$$

Using the Lagrange formulation, the boom's nonlinear equation of motion was obtained using

$$[\mathbf{M}(\underline{\mathbf{z}})]\ddot{\underline{\mathbf{z}}} = f(\underline{\mathbf{z}}, \dot{\underline{\mathbf{z}}}) + [\boldsymbol{\Lambda}_{\mathrm{act}}(\underline{\mathbf{z}})]^{\mathrm{T}}\underline{\mathbf{F}}_{\mathrm{act}}(t) \tag{2}$$

where $[\mathbf{M}(\underline{\mathbf{z}})]$ represents the inertial contribution; $f(\underline{\mathbf{z}}, \dot{\underline{\mathbf{z}}})$ contains all the nonlinear damping, elastic and gravitational terms; $\underline{\mathbf{F}}_{\mathrm{act}}$ represents the large motion actuator forces and $[\boldsymbol{\Lambda}_{\mathrm{act}}(\underline{\mathbf{z}})]$ represents the kinematic relationship between the actuator length $\underline{\boldsymbol{\rho}}$ and the independent coordinates vector ($\underline{\mathbf{z}}$).

Eq. (2) is a nonlinear equation because all the matrices depend on the motion variables and in particular on the segment configuration.

To study the vibration problem and obtain system eigenvalues, the nonlinear equation can be evaluated and linearized in each boom configuration. In a generic configuration of the system "$\underline{\mathbf{z}} = \underline{\mathbf{z}}_i$", Eq. (2) becomes

$$[\mathbf{M}_i] \cdot \delta\ddot{\underline{\mathbf{z}}}_i + [\mathbf{R}_i] \cdot \delta\dot{\underline{\mathbf{z}}}_i + [\mathbf{K}_i] \cdot \delta\underline{\mathbf{z}}_i = \underline{\mathbf{f}}_g(\underline{\mathbf{z}}_i) + [\boldsymbol{\Lambda}_i]^{\mathrm{T}}\underline{\mathbf{F}}_{\mathrm{act}} \tag{3}$$

where $[\mathbf{M}_i]$ and $[\mathbf{K}_i]$, respectively, represent the inertial and elastic matrices, considering both the structural term and the actuator contribution; the damping term $[\mathbf{R}_i]$ is assumed to be proportional to the elastic and inertial terms. The proportional coefficients are estimated from experimental data; $\underline{\mathbf{f}}_g(\underline{\mathbf{z}}_i)$ represents the constant contribution of the gravitational term.

Owing to the low segment rotation speed, centrifugal and Coriolis terms were neglected.

The following paragraph presents and numerically/experimentally investigates a control logic for reducing the structural vibrations.

3. Active control

In operating conditions, the system described earlier is subjected to a generic large motion which causes, because of the high flexibility of the segments, significant vibration levels. To suppress these vibrations ($\delta\underline{\mathbf{z}}$), this paper proposes applying a control action using the same actuators used to move the individual segments. As shown in Fig. 3, control forces $\underline{\mathbf{u}}_c$ work in parallel with the large motion forces $\underline{\mathbf{F}}_{\mathrm{act}}$.

The vibration control logic adopted is based on an independent modal approach [2]. Following this approach, the control action is calculated starting from the system vibratory state and a suitably defined gain matrix. In particular the vibratory state is described by a set of modal coordinates representing the system dynamics in the frequency range of interest. The modal coordinates, which for a generic application cannot be measured directly (unless we use distributed sensors [6]), have to be estimated by a modal observer. Below, the individual steps are analyzed in depth.

The control synthesis can be calculated starting from Eq. (3), without considering the gravitational and external forces terms because these contributions do not modify the value of the poles:

$$[\mathbf{M}_i] \cdot \delta\ddot{\underline{\mathbf{z}}}_i + [\mathbf{R}_i] \cdot \delta\dot{\underline{\mathbf{z}}}_i + [\mathbf{K}_i] \cdot \delta\underline{\mathbf{z}}_i = [\boldsymbol{\Lambda}_i]^{\mathrm{T}}\underline{\mathbf{u}}_c \tag{4}$$

The aim of the control force $\underline{\mathbf{u}}_c$ is to increase the system's damping ratio in order to reduce vibrations by imposing new values $\underline{\boldsymbol{\lambda}}_c$ for the system's original eigenvalues $\underline{\boldsymbol{\lambda}}$. In particular the real part of the system's eigenvalues was increased, while

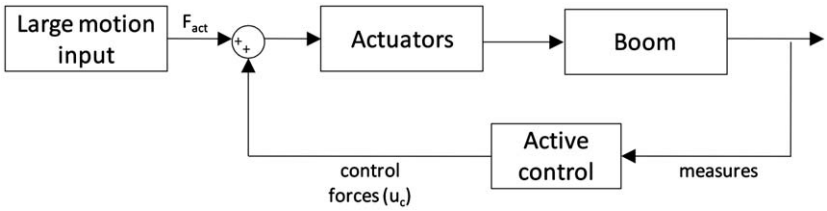

Fig. 3. Block diagram of the active control logic.

the imaginary part remained unchanged so as to avoid having to use significant control forces and imposing additional mechanical fatigue stress on the boom material.

This could be achieved using a state-space control method, such as pole placement. Considering a generic second-order mechanical system and defining the state-space vector

$$\underline{\mathbf{x}} = \begin{Bmatrix} \delta\underline{\dot{\mathbf{z}}}_i \\ \delta\underline{\mathbf{z}}_i \end{Bmatrix} \tag{5}$$

Eq. (4) can be written as

$$\underline{\dot{\mathbf{x}}} = \begin{bmatrix} -[\mathbf{M}_i]^{-1}[\mathbf{R}_i] & -[\mathbf{M}_i]^{-1}[\mathbf{K}_i] \\ [\mathbf{I}] & [\mathbf{0}] \end{bmatrix} \underline{\mathbf{x}} + \begin{bmatrix} [\mathbf{M}_i]^{-1}[\Lambda_i]^{\mathrm{T}} \\ [\mathbf{0}] \end{bmatrix} \underline{\mathbf{u}}_c = [\mathbf{A}_i]\underline{\mathbf{x}} + [\mathbf{B}_i]\underline{\mathbf{u}}_c \tag{6}$$

In a second-order system, the eigenvector matrix of the uncontrolled system can be written as [14]

$$[\mathbf{U}_i] = \begin{bmatrix} [\mathbf{\Phi}_i][\lambda_i] \\ [\mathbf{\Phi}_i] \end{bmatrix} \tag{7}$$

where $[\lambda_i]$ represents the eigenvalue diagonal matrix of the state-matrix $[\mathbf{A}_i]$; $[\mathbf{\Phi}_i]$ contains, in its columns, information on the modal shapes of the system.

Defining the control law as

$$\underline{\mathbf{u}}_c = -[\mathbf{G}_i]\underline{\mathbf{x}} \tag{8}$$

Eq. (6) becomes

$$\underline{\dot{\mathbf{x}}} = [[\mathbf{A}_i] - [\mathbf{B}_i][\mathbf{G}_i]]\underline{\mathbf{x}} = [\mathbf{A}_{i,c}]\underline{\mathbf{x}} \tag{9}$$

In the pole position control strategy, the gain matrix $[\mathbf{G}_i]$ can be chosen so that the state matrix of the controlled system $[\mathbf{A}_{i,c}]$ has the desired eigenvalues $\underline{\lambda}_c$. For a multi-input system, other conditions can be imposed to obtain an analytical formulation for $[\mathbf{G}_i]$. For example the controlled system eigenvectors can be set equal to those of the uncontrolled system ($[\mathbf{\Phi}_{i,c}] = [\mathbf{\Phi}_i]$). In this case, $[\mathbf{G}_i]$ can be calculated from an eigenvalue problem of $[\mathbf{A}_{i,c}]$

$$([\mathbf{A}_i] - [\mathbf{B}_i][\mathbf{G}_i])[\mathbf{U}_{i,c}] = [\mathbf{U}_{i,c}][\lambda_{i,c}] \tag{10}$$

where the matrix $[\mathbf{U}_{i,c}]$ is defined by Eq. (7), with $[\mathbf{\Phi}_{i,c}] = [\mathbf{\Phi}_i]$ and eigenvalues $[\lambda_{i,c}]$.

Remembering Eq. (10), it is possible to invert this relationship, obtaining the independent modal control gain formulation in state-space approach

$$[\mathbf{G}_i] = [[\overline{\mathbf{B}}_i]^{-1} \ [\mathbf{0}]]([\mathbf{A}_i] - [\mathbf{U}_{i,c}][\lambda_{i,c}][\mathbf{U}_{i,c}]^{-1}) \tag{11}$$

where $[\overline{\mathbf{B}}_i]$ represents the upper part of $[\mathbf{B}_i]$ (the lower part, for a mechanical second-order system, is equal to zero). This formulation can be applied to any second-order system that has as many inputs as degrees of freedom ($[\overline{\mathbf{B}}_i]$ must be square). In addition, the controllability of the system must be guaranteed.

As previously described, in the present work the motion equation was obtained using FEM discretization of the links. This means that the variable vector $\underline{\mathbf{z}}$ contains, as mentioned in par. 2, all the nodal displacement of the structure, and its dimension is not compatible with the formulation presented in Eq. (11), because only three actuators are available on the boom. Moreover, it should be considered that the structure dynamic is ruled only by the first modes, because high frequency modes usually have higher damping ratios and they can hardly be excited.

For this reason a reduced modal system needs to be defined to describe boom motion using a limited set of coordinates, taking into account the well-known problem of spillover.

3.1. Independent modal control

Defining the complete modal coordinates vector as $\underline{\mathbf{q}}_{\mathbf{tot}}$ and the partition of $\underline{\mathbf{q}}_{\mathbf{tot}}$ containing only the m modal coordinates considered as $\underline{\mathbf{q}}_{\mathbf{z}}$, we can perform the coordinate change

$$\delta\underline{\mathbf{z}} = [\boldsymbol{\varphi}_{i,\mathrm{tot}}]\underline{\mathbf{q}}_{\mathbf{tot}} \simeq [\boldsymbol{\varphi}_i]\underline{\mathbf{q}}_z \tag{12}$$

where $[\boldsymbol{\varphi}_{i,\mathrm{tot}}]$ represents the eigenvector matrix of $([\mathbf{M}_i]^{-1}[\mathbf{K}_i])$, while $[\boldsymbol{\varphi}_i]$ is a partition of $[\boldsymbol{\varphi}_{i,\mathrm{tot}}]$ containing only the eigenvectors of the modes considered.

Applying Eq. (12) to Eq. (4), the motion equation becomes a set of independent modal equations

$$[\mathbf{m}_i]\ddot{\underline{\mathbf{q}}}_z + [\mathbf{r}_i]\dot{\underline{\mathbf{q}}}_z + [\mathbf{k}_i]\underline{\mathbf{q}}_z = [\boldsymbol{\varphi}_i]^{\mathrm{T}}[\boldsymbol{\Lambda}_i]^{\mathrm{T}}\underline{\mathbf{u}}_c \tag{13}$$

where $[\mathbf{m}_i]$, $[\mathbf{r}_i]$ and $[\mathbf{k}_i]$ are $m \times m$ diagonal matrices, obtained by

$$[\mathbf{m}_i] = [\boldsymbol{\varphi}_i]^{\mathrm{T}}[\mathbf{M}_i][\boldsymbol{\varphi}_i], \ldots \tag{14}$$

It should be noted that Eqs. (13) and (14) are only valid for systems with real modes. Anyway the examined system damping is very small and its modes can be assumed real.

As an example, Fig. 4 shows the first (a) and the second (b) mode shape for the boom in the horizontal configuration.

To apply the state-space control approach to the reduced modal system, Eq. (13) can be written in state-space form:

$$\dot{\underline{\mathbf{q}}} = \begin{bmatrix} -[\mathbf{m}_i]^{-1}[\mathbf{r}_i] & -[\mathbf{m}_i]^{-1}[\mathbf{k}_i] \\ [\mathbf{I}] & [\mathbf{0}] \end{bmatrix}\underline{\mathbf{q}} + \begin{bmatrix} [\mathbf{m}_i]^{-1}[\boldsymbol{\varphi}_i]^{\mathrm{T}}[\boldsymbol{\Lambda}_i]^{\mathrm{T}} \\ [\mathbf{0}] \end{bmatrix}\underline{\mathbf{u}}_c = [\mathbf{A}_q]\underline{\mathbf{q}} + [\mathbf{B}_q]\underline{\mathbf{u}}_c \tag{15}$$

where

$$\underline{\mathbf{q}} = \begin{Bmatrix} \dot{\underline{\mathbf{q}}}_z \\ \underline{\mathbf{q}}_z \end{Bmatrix} \tag{16}$$

Applying (11) to (15), the gain matrix $[\mathbf{G}_m]$ can be calculated, and the control force $\underline{\mathbf{u}}_c$ is defined as

$$\underline{\mathbf{u}}_c = -[\mathbf{G}_m] \cdot \underline{\mathbf{q}} \tag{17}$$

In this way, Eq. (15) becomes

$$\dot{\underline{\mathbf{q}}} = ([\mathbf{A}_q] - [\mathbf{B}_q][\mathbf{G}_m])\underline{\mathbf{q}} = [\mathbf{A}_{q,c}]\underline{\mathbf{q}} \tag{18}$$

The disadvantage of the state-space approach is that the gain matrix values lose physical meaning. For this reason, the modal control law proposed has been calculated imposing that the term $[\boldsymbol{\varphi}_i]^{\mathrm{T}}[\boldsymbol{\Lambda}_i]^{\mathrm{T}}\underline{\mathbf{u}}_c$ of (13) does not couple the system modes and leads to an increase of the system damping ratio:

$$[\boldsymbol{\varphi}_i]^{\mathrm{T}}[\boldsymbol{\Lambda}_i]^{\mathrm{T}}\underline{\mathbf{u}}_c = [\mathbf{g}_v] \cdot (\dot{\underline{\mathbf{q}}}_{\mathrm{ref}} - \dot{\underline{\mathbf{q}}}_z) + [\mathbf{g}_p] \cdot (\underline{\mathbf{q}}_{\mathrm{ref}} - \underline{\mathbf{q}}_z) \tag{19}$$

where $\underline{\mathbf{q}}_{\mathrm{ref}}$ and $\dot{\underline{\mathbf{q}}}_{\mathrm{ref}}$ are the reference modal coordinates vectors, and are set to zero because the aim of control is to eliminate vibrations. In this formulation $[\mathbf{g}_v]$ and $[\mathbf{g}_p]$ have a precise physical meaning, because they represent, respectively, the increase in stiffness and damping ratio brought about by the control. To ensure independent modal control they must be diagonal, so that the control law provides an independent stiffness and damping contribution on each mode, keeping the same eigenvectors as the uncontrolled system. This condition can be obtained only if the number of actuators is equal to the number of considered modal coordinates ($n_a = m$). In addition, the system must be controllable, so any row or

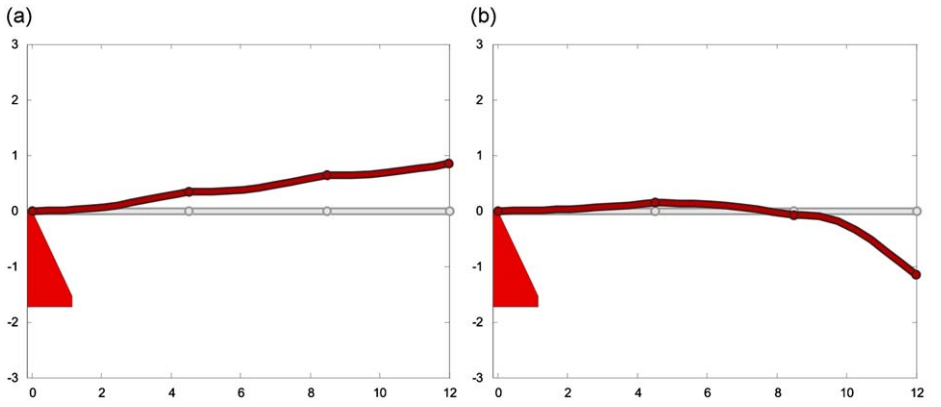

Fig. 4. Numerical modal analysis of the boom in horizontal configuration: first (a) and second (b) mode shape.

column of $[\boldsymbol{\varphi}_i]^T[\boldsymbol{\Lambda}_i]^T$ must be non-zero. This means that at least one control force must have a non-zero contribution on every mode and each control force must act on at least one mode.

The control force can be calculated as

$$\underline{\mathbf{u}}_c = ([\boldsymbol{\varphi}_i]^T[\boldsymbol{\Lambda}_i]^T)^{-1}(-[\mathbf{g}_v]\cdot\underline{\dot{\mathbf{q}}}_z - [\mathbf{g}_p]\cdot\underline{\mathbf{q}}_z) = -[\mathbf{G}_v]\cdot\underline{\dot{\mathbf{q}}}_z - [\mathbf{G}_p]\cdot\underline{\mathbf{q}}_z \tag{20}$$

selecting $[\mathbf{G}_v]$ and $[\mathbf{G}_p]$ so as to obtain the controlled system eigenvalues desired. In particular $[\mathbf{G}_p]$ was set to zero to keep the same natural frequencies as the uncontrolled system.

3.2. The modal observer

Assuming that the exact modal coordinates are known, the method proposed guarantees a completely decoupled modal control and avoids spillover problems, even if the number of controlled modes is smaller than the number of structure modes.

However, in most flexible structure control applications the modal coordinates are unknown and so have to be estimated using a modal observer or filter [3]. In this case the control system is not immune to observation spillover problems, as shown later. The implemented modal observer scheme is shown in Fig. 5.

According to Eq. (18), the observer equation can be written as

$$\dot{\underline{\hat{\mathbf{q}}}} = [\mathbf{A}_{q,c}]\underline{\hat{\mathbf{q}}} + [\mathbf{G}_o](\underline{\boldsymbol{\mu}} - \underline{\hat{\boldsymbol{\mu}}}) \tag{21}$$

where $[\mathbf{A}_{q,c}]$ is the state-space matrix of the controlled reduced modal system; $[\mathbf{G}_o]$ is the observer gain matrix, which will be defined later; $\underline{\hat{\mathbf{q}}}$ represents the estimated modal coordinates; and $\underline{\boldsymbol{\mu}}$ and $\underline{\hat{\boldsymbol{\mu}}}$, respectively, represent the measures and estimated measures vectors. $\underline{\boldsymbol{\mu}}$ is an observer input, while $\underline{\hat{\boldsymbol{\mu}}}$ is defined by

$$\underline{\hat{\boldsymbol{\mu}}} = [\mathbf{C}]\underline{\hat{\mathbf{q}}} \tag{22}$$

The values of $[\mathbf{C}]$, which link the estimated measures vector to the observer inputs, depend on sensor type (accelerometer, position sensors, strain gauges, etc.).

Considering Eq. (22), the observer equation (21) becomes

$$\dot{\underline{\hat{\mathbf{q}}}} = ([\mathbf{A}_{q,c}] - [\mathbf{G}_o][\mathbf{C}])\underline{\hat{\mathbf{q}}} + [\mathbf{G}_o]\underline{\boldsymbol{\mu}} = [\mathbf{A}_{q,o}]\underline{\hat{\mathbf{q}}} + [\mathbf{G}_o]\underline{\boldsymbol{\mu}} \tag{23}$$

To define the matrix $[\mathbf{C}]$ it is important to underline that, in this paper, the sensors used to estimate modal coordinates were accelerometers. We can define

$$\mu^i = \underline{\mathbf{E}}_i^T \cdot \delta\underline{\ddot{\mathbf{z}}} \tag{24}$$

where $\underline{\mathbf{E}}_i^T$ is a row vector that represents the relationship between the i-th accelerometer measure and the independent coordinates (second-order time derivatives). Starting from (24), applied to the estimated state, and considering Eqs. (12) and (15), each row of the $[\mathbf{C}]$ matrix can be defined as

$$\underline{\mathbf{C}}_i^T = (\underline{\mathbf{E}}_i^T)[\boldsymbol{\varphi}_k][\overline{\mathbf{A}}_{q,c}] \tag{25}$$

where $[\overline{\mathbf{A}}_{q,c}]$ represents the upper part of the state space matrix $[\mathbf{A}_q]$ defined in Eq. (18).

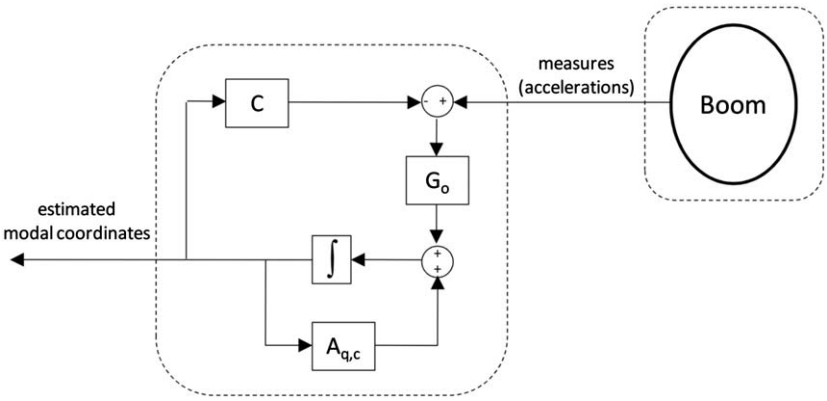

Fig. 5. Block diagram of the modal observer.

Finally [**C**] can be obtained combining the contributions as

$$[\mathbf{C}] = \begin{bmatrix} \underline{\mathbf{C}}_1^{\mathrm{T}} \\ \vdots \\ \underline{\mathbf{C}}_1^{\mathrm{T}} \\ \vdots \end{bmatrix} \tag{26}$$

Now it is possible to define the last term of the observer, the gain matrix $[\mathbf{G}_o]$, which is calculated using the pole placement method. In this case a single-input observer (one accelerometer) has been implemented and the gain matrix $[\mathbf{G}_o]$ has been calculated as

$$[\mathbf{G}_o] = [\mathbf{T}]^{-1}(\underline{\mathbf{a}}_o - \underline{\mathbf{a}}) \tag{27}$$

where the column vectors $\underline{\mathbf{a}}$ and $\underline{\mathbf{a}}_o$ contain the characteristic polynomial coefficients of the reduced modal state-space matrix and observer state-space matrix ($[\mathbf{A}_{q,c}]$ and $[\mathbf{A}_{q,o}]$), while $[\mathbf{T}]^{-1}$ is known as the Toeplitz matrix [15].

4. Numerical-experimental analysis

In the previous paragraph the vibration control logic was defined. To test the adopted solution, a numerical and experimental campaign was carried out. The test rig, introduced in par. 2, was fitted with

- three load cells, to read total actuator forces;
- three LVDT sensors, to obtain boom configuration; and
- one accelerometer used as the observer input and the boom vibration indicator, located at the end of the last segment.

As mentioned above, the motion of the system is described by a nonlinear Eq. (2). For this reason all control matrices need to be updated at every step to make the control logic rigorous. This updating can be easily reproduced in the numerical simulations, where there are no limits due to real-time issues.

However, the experimental application requires real-time calculation of control matrices, which means that each step must be completed in about 1 ms. Normal microprocessors do not have enough power or speed to handle this time scale, so an approximation must be applied. In any case, considering that the rotation speed of the segment (and so the matrix variation) is lower with respect to the controller dynamic, this approximation does not compromise control efficiency and two possible approaches can be adopted.

The first consists in calculating control matrices every n time steps, using the control board in a multi-tasking mode. A faster method calculates the control forces every time step while the other method calculates them at longer intervals.

The second approach is to pre-calculate the matrices for a discrete set of boom configurations. In this way, at every time step, the software simply needs to extract the nearest configuration matrices using linear interpolation. The actual boom configuration, as mentioned, can be determined from the actuator LVDT output. The limit of this solution is the memory available on the control board.

Considering the small amount of memory required by the present application, this second method (Fig. 6) was preferred and implemented.

Fig. 7 shows the pole diagrams of the system with and without modal control (three modes). The controlled system and observer pole are set as follows:

- the imaginary part of each controlled and observed pole is set equal to the imaginary part of the uncontrolled system. This is because we are not interested in modifying the system frequencies since this is not the aim of the present work and would lead to high control forces. As mentioned, a control force increase could lead to high mechanical stress and fatigue problems;
- the real part of each controlled and observed pole is placed, respectively, equal to 10 and 30 percent of the corresponding imaginary one, in order to set the controlled system damping ratio higher than that of the uncontrolled boom; these values were chosen to maximize the closed-loop system damping ratio.

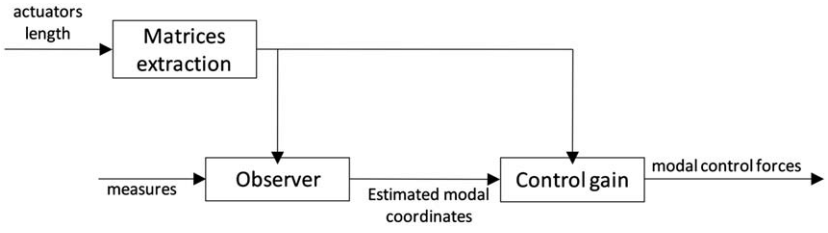

Fig. 6. Block diagram of the control implementation scheme.

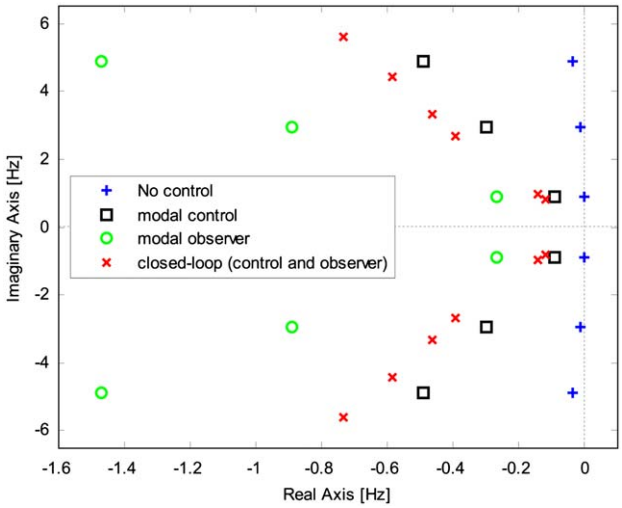

Fig. 7. Controlled system and observer eigenvalues position.

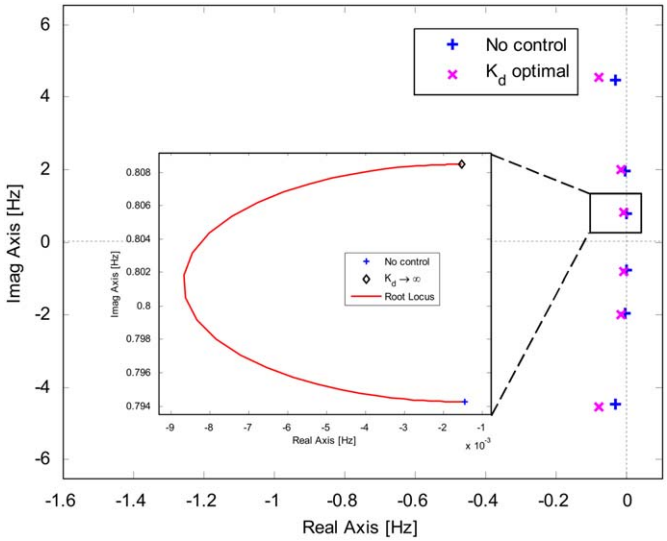

Fig. 8. Eigenvalues position with derivative control; root locus for different values of K_d (in the zoomed window).

Fig. 7 shows the imposed pole position of the modal controller and the observer with respect to the uncontrolled system poles. We can see that the closed loop poles are not in the place they were designed to be, but in an intermediate position. This is because of the combination between the control and observer loop.

For comparison, the possibility of using a co-located control force was analyzed. This solution is the simplest one, because it only requires the measurement of the actuator length $\underline{\boldsymbol{\rho}}$ and is the most natural solution for adding damping to the system. The resulting control force, where $[\mathbf{K}_d]$ is a diagonal matrix

$$\underline{\mathbf{u}}_c = [\mathbf{K}_d] \cdot (\dot{\underline{\boldsymbol{\rho}}}_{\text{ref}} - \dot{\underline{\boldsymbol{\rho}}}) \tag{28}$$

consists of a co-located derivative control, that increases the total damping of the system by adding a damping contribution on the boom actuators. This solution is simpler than modal control. In fact it requires low computational effort and does not compromise system stability.

However, this solution does not provide a large increase in the damping ratio. In fact this derivative action only works on actuator vibrations, without considering the vibrations of the segments due to their flexibility.

As a consequence, even after optimization, only a small damping ratio increase is achieved. Fig. 8 shows the root locus of the boom in the horizontally aligned configuration and the poles position with optimal derivative gains.

4.1. Numerical analysis

This paragraph presents some numerical results. All the simulations refer to the numerical model of the test rig that was used for the experiments. All the results (with and without vibration control) refer to the same large movement of the boom (Fig. 9).

Fig. 10 compares the damping effect of the derivative term of co-located action and modal control. The acceleration of the end of the third segment is considered as indicating control performance.

On the left, the figure shows the acceleration time history during the large motion described in Fig. 9. The time history also includes static acceleration due to gravity.

On the right it shows, on a logarithmic scale, the acceleration spectrum with the application of an external force on the first segment end. This simulation was carried out in the final configuration of the large motion shown in Fig. 9. The external force consists of a frequency sweep up to 6 Hz, that involves the first three natural frequencies of the structure. The figure shows that modal control causes a large reduction of vibrations near the controlled natural frequencies. However, system response increases between these.

In any case, as Table 1 also presents, modal control can ensure a large increment in the boom damping ratio.

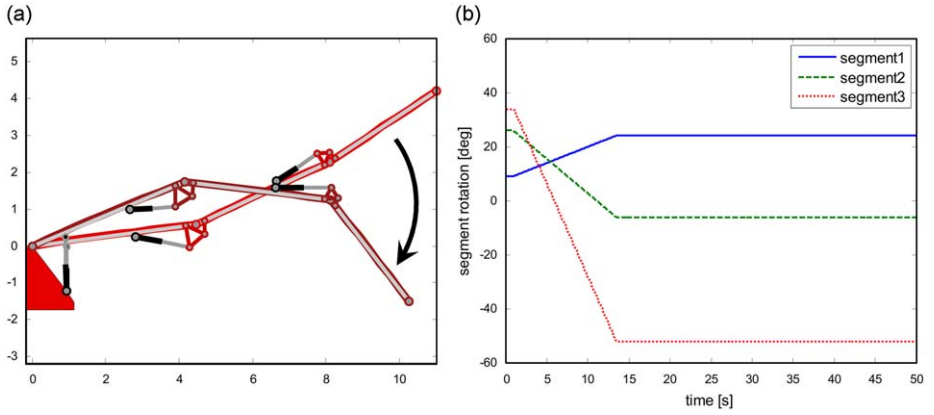

Fig. 9. Large motion reference for the boom segments; starting and final configuration (a), segment rotation time history (b).

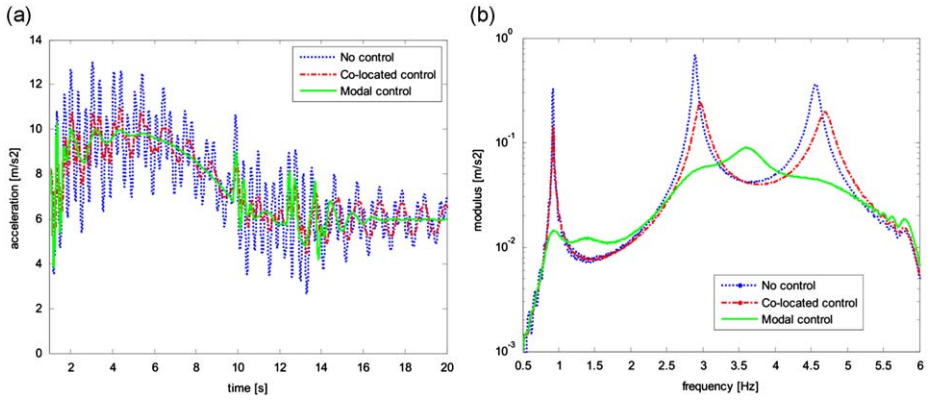

Fig. 10. Numerical acceleration of the end of the third boom segment; time history (a) and spectrum (b).

Table 1
Comparison between the damping ratios of the first three modes of the boom in horizontal configuration with and without modal control.

Damping ratios (%)	No control	Co-located control	Modal control
Mode 1	0.19	1.10	14.4
Mode 2	0.42	1.20	13.9
Mode 3	0.73	1.72	13.1

4.2. Experimental results

This paragraph presents the results obtained on the test rig. The rig is composed of three segments, as shown in Fig. 11.

As in the numerical case, the acceleration of the end of the third segment is considered to estimate control performance.

Fig. 12 shows the experimental results, obtained reproducing the same conditions as in the numerical simulations (movement, control parameter, measurement instruments).

We can see that the test rig boom is subjected to observation spillover problems [9]. In particular, we can see that, in this application, control forces make the fifth structure mode (the second uncontrolled one) unstable. This means that this mode cannot be ignored in the boom dynamic, and must be included in the reduced system definition. This phenomenon is not highlighted by the numerical simulations, where control matrices calculation is rigorous. In fact exactly the same system was used both in the control synthesis and in the numerical motion integration. Moreover it must be considered that the proportional damping factors of the numerical model has been calibrated to correctly reproduce the first three modes damping ratios. This choice may have led to an over-estimation of the damping at the higher frequencies, increasing

Fig. 11. A picture of the test rig.

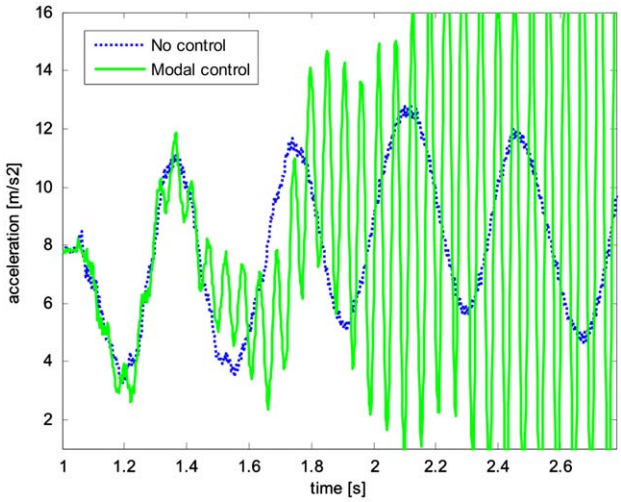

Fig. 12. Experimental acceleration of the end of the third boom segment with 3-modes observer; time history.

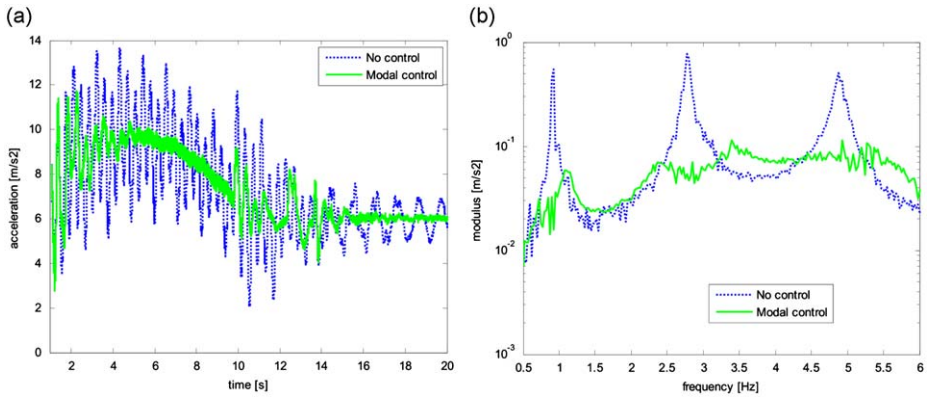

Fig. 13. Experimental acceleration of the end of the third boom segment with 5-modes observer; time history (a) and spectrum (b).

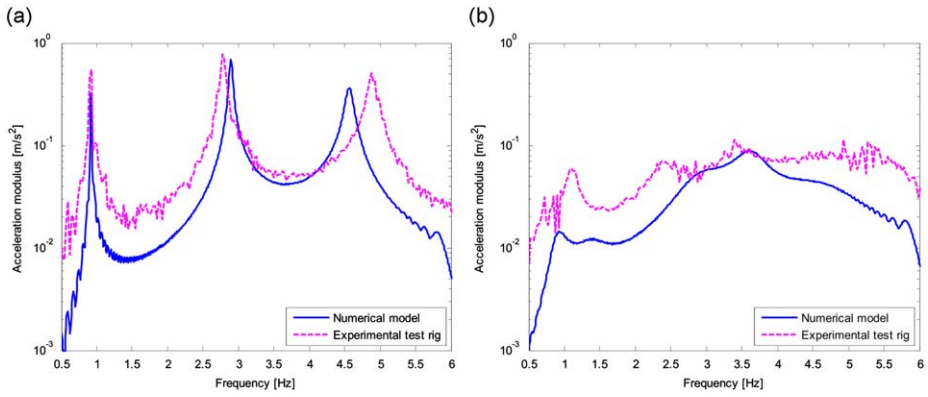

Fig. 14. Numerical-experimental spectra comparison without (a) and with (b) modal control.

the numerical integration stability. On the other side, in the experimental tests, the differences between the model and the experimental test rig lead to a non-rigorously independent modal control law.

As a consequence, to solve the problem, a five modes observer was implemented, to avoid observation spillover problems, while the control gain matrix remained the same, since only the feed-back of the first three modes was considered. Fig. 13 shows the experimental results using the improved control settings. We can see that spillover problems were resolved and good agreement with the numerical data was obtained.

In order to complete the numerical-experimental analysis, in Fig. 14 a comparison is shown.

5. Conclusions

In this paper a control strategy was implemented to suppress the vibrations induced in a nonlinear highly flexible boom by its large motion. For this kind of structure the modal solution remains an attractive one for modelling the system dynamics with a reduced number of degrees of freedom in a focused range of frequencies. As a consequence the nonlinear active control logic adopted is based on the independent modal control theory, illustrated using the state-space formulation. In the same way, a modal observer was implemented to estimate the non-measurable modal coordinates. The control force is applied to the system through the same hydraulic actuators responsible for the boom's large motion.

First this methodology was tested using numerical simulation, showing that an increase of the damping ratio of up to about 15 percent could be achieved without affecting the large motion and reducing material stress during operation.

Finally a test rig was created and the methodology was experimentally validated. The experiments highlighted the need to increase the number of observed modes to avoid instability problems due to spillover.

References

[1] M.J. Balas, Active control of flexible systems, *Journal of Optimization Theory and Applications* 25 (3) (1978) 415–436.
[2] L. Meirovitch, Comparison of control techniques for large flexible systems, *Journal of Guidance, Control, and Dynamics* 6 (4) (1983) 302–310.
[3] L. Meirovitch, H. Baruh, Implementation of modal filters for control of structures, *Journal of Guidance Control, and Dynamics* 8 (6) (1985) 707–716.

[4] A. Baz, S. Poh, Experimental implementation of the modified independent modal space control method, *Journal of Sound and Vibration* 139 (1) (1990) 133–149.
[5] Y.H. Lin, C.L. Chu, A new design for independent modal space control of general dynamic systems, *Journal of Sound and Vibration* 180 (1995) 351–361.
[6] C.K. Lee, F.C. Moon, Modal sensors/actuators, *Journal of Applied Mechanics, Transactions ASME* 57 (2) (1990) 434–441.
[7] X. Zhang, H. Liu, W. Cao, Active vibration control of flexible mechanisms, *Chinese Journal of Mechanical Engineering* 32 (1) (1996) 9–16.
[8] S. Changjian, Z. Xianmin, S. Yunwen, Complex mode active vibration control of high-speed flexible linkage mechanisms, *Journal of Sound and Vibration* 234 (3) (2000) 491–506.
[9] D.J. Inman, Active modal control for smart structures, *Philosophical Transactions of the Royal Society Series A* 359 (1778) (2001) 205–219.
[10] G.R. Skidmore, W.L. Hallauer Jr., Modal-space active damping of a beam-cable structure: theory and experiment, *Journal of Sound and Vibration* 101 (2) (1985) 149–160.
[11] Y.A. Khulief, Vibration suppression in rotating beams using active modal control, *Journal of Sound and Vibration* 242 (4) (2001) 681–699.
[12] Y.-H. Lin, Y.-K. Tsai, Nonlinear vibrations of timoshenko pipes conveying fluid, *International Journal of Solids and Structures* 34 (23) (1997) 2945–2956.
[13] A.A. Shabana, Flexible multibody dynamics: review of past and recent developments, *Multibody System Dynamics* 1 (2) (1997) 189–222.
[14] L. Meirovitch, *Dynamics and Control of Structures*, Wiley, New York, 1990 ISBN 0471628581.
[15] B. Friedland, *Control System Design*, McGraw-Hill, New York, 1986 ISBN 0070224412.